ORIGINAL RESEARCH PAPER
Volume - 11 | Issue - 11 | November - 2022 | PRINT ISSN No. 2277 - 8179 | DOI : 10.36106/ijsr
INTERNATIONAL JOURNAL OF SCIENTIFIC RESEARCH

LUNG DEPOSITION RATE AND AEROSOL CHARACTERISTICS OF A NANO AEROSOL NOZZLE WITH DEXAMETHASONE SOLUTION

Veterinary Science

Hans Peter Zarfl* Auenstrasse 45, 9400 Wolfsberg, Austria (EU). *Corresponding Author

Pierre Madl Department of Biosciences & Medical Biology / Paris Lodron University Salzburg - Austria (EU).

ABSTRACT

A nanoaerosol nozzle was designed and the generated aerosol consisting of a diluted dexamethasone solution was measured with Scanning Mobility Particle Sizer (SMPS). The obtained aerosol concentration was fed into the IDEAL lung deposition model for to calculate expected deposition in a human lung. Measurements and calculation clearly show that a substantial fraction reaches the alveolar section of the lungs. Given the generated particle inventory in the nano-size range, the tested nozzle appears to have specific advantages for deposition in deeper pulmonary region over existing "out of the shelf" devices. Considering therapeutic applications, the high share of nano-sized particles make it possible to reduce dosage without compromising the therapeutic effects. While most devices currently in use achieve only about 10 % lung deposition efficiency, with the bulk of the aerosolized fraction trapped in the extra-thoracic region. With this novel aerosolizer it is possible to reduce oropharyngeal deposition to about 4,78-5.97 %, leaving 25.6-25.5 % being deposited in the deeper lung, while the remaining fraction being expelled with the exhalation bolus.

KEYWORDS

INTRODUCTION

The most commonly used aerosolizers for bio-medical applications – both professional devices as well as hand-held puffing devices – focus on the maximization of drug deposition in terms of mass. Thus, most of these devices are tuned to maximize mass deposition (Mass Median Aerosol Diameter, MMD) around 3-6 µm (Knoch & Finlay, 2002). Portable, pressurized dose inhalators as commonly used for asthmatics or COPD patients, disperse droplets usually within a much larger size range such as 10-50 µm (Adjei, 2002), whereas stationary devices do only slightly better by generating aerosols in the 1-10 µm range (Hickey & Swift, 2001). The technology employed for aerosol generation and deposition in the respiratory tract typically relies on i) jet-venturi-based nebulization using compressed air yielding <5-6 µm particles, ii) vibrating membrane mesh-type yielding >2 µm particles, iii) ultrasonic nebulization for aqueous aerosols <5 µm and iv) Electrodynamic devices which charge the aerosol (Knoch & Finlay, 2002; Berlinski & Willis, 2013) generating a bulk particle fraction around 40-50 6 µm (Rosell-Llompart et al., 2018) and dry-powder inhalators that make advantage of the freeze-dried pharmaceutical agent that is present as a easily airborne powder (Sorino et al., 2020) in a size range of 1-10 µm (Hickey, 2002, Telko, 2009). In order to be inhalable, all these devices need to operate under low-flow conditions at around 3-6 L/min (Knoch & Finlay, 2002).

A drawback of these concepts can be easily understood when looking at their mode of operation as the typical aerosol generator in clinical applications are of those ones operating in constant-output (or un-vented) mode leading to at least 50 % of the aerosol being wasted to the environment. It becomes slightly better when breath-enhanced (or vented) modes are used and much better than breath-activated nebulization is employed. In ultrasonic nebulizers, aspect like excessive heating of the liquid to be aerosolized (due to contact with the oscillating piezo membrane) can alter drug properties altogether (Knoch & Finlay, 2002), while cavitation events (high pressure and temperature gradients during sonoluminescence) can result even in chemical disintegration of sensitive compounds (Young, 1999). In addition of gaining an additional charge, ultrasonic nebulizers also emit a substantial quantity of "ultraweak" photons in the order of >200 cts/s within the visible range (Yan, 2001).

In terms of charge build-up, especially with electrodynamic devices, the loaded charge imprinted onto the aerosol can drastically alter lung deposition properties (Hussain et al., 2012). In addition, and due to the high potential (several kV) applied during electrodynamic atomization, the generated Taylor cone yielding a steady flow of atomized droplets can have detrimental effects on sensitive therapeutic agents that do not tolerate charging at al (Rosell-Llompart et al., 2018).

Why is there a need for novel class of aerosolizers?

As depicted in Figure 1a, aerosols are found in a wide range as these can emerge from gaseous precursors or from mechanical processes, which are usually several orders of magnitude larger. An aqueous aerosol such as cloud condensation nuclei are found in the size range of about 200 nm – which under homo- or heterogenous nucleation conditions – result in cloud or fog droplets of 1-10 mm in size that are easily translocatable as an electrodynamic "ensemble" (Madl et al., 2013). Decoherence of these ensembles induces larger droplets formation (<2 mm), which no longer can remain airborne and rapidly precipitate due to the gravitational pull as ice crystals and eventually as rain (Lutgens & Tarbuck, 2010). Thus, the size range of the entire aqueous particle inventory stretches over five orders of magnitude revealing an underlying fractal nature (Christensen & Driver, 2021). The same fractal pattern is also visible in the respiratory tract, in that the self-similar branching structure of the bifurcating bronchi / achieve the gradual filtering effect of the inhaled aerosol plume by gradually separating the larger sibling from the ultra-fine aqueous particles as the inhaled bolus penetrates deeper and deeper into the lungs. In terms of proper alveolar penetration, a therapeutic aerosol targeting the alveolar regime should be grouped predominantly within the nucleation regime (at the far-end of Figure 1a; i.e. <1 mm) minimizing filtering effects due to impaction as well as gravitational settling within the coarser airways and consequently enabling diffusion and charge-induced deposition within the gas-exchange region of the lung. Being able to generate ultrafine aerosols with a nozzle as depicted in Figure 2 it is thus possible to increase deep lung penetration all the way to the alveolar regime, thereby inducing an organismic-wide effect as a large part of the nano-sized fraction not only penetrates alveoli, but more so trespasses well into the capillary structures of the pulmonary tissue to become dispersed via the circulatory system inducing an organismic-wide effect. So far, most therapeutic aerosol generators target the thoracic regime and usually do not operate in the sub-micrometer range and as such generate aerosols >1 mm facilitating gravitational settling, sedimentation as well as impaction within the larger respiratory ducts (see Figure 1b).

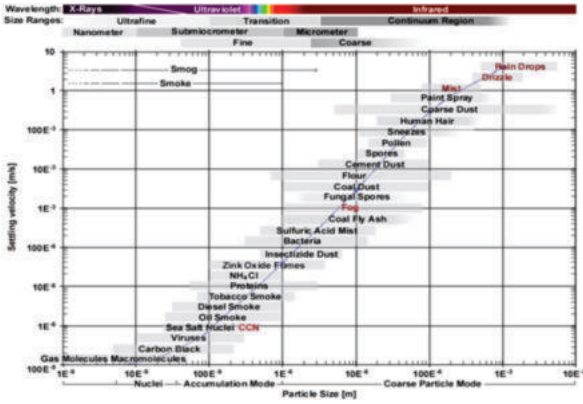

Fig. 1a Comparison of selected aerosol classes and their particle sizes

ranges versus sedimentation rates. The upper abscissa depicts a rough classification of the corresponding electromagnetic spectrum, including the narrow band of "visible light", clearly denoting the threshold between optically perceivable particles and none (Madl, 2012). Reddish letters denote aqueous particles, CCN, cloud condensation nuclei.

Moreover, ultrafine-particle generation is not just a crucial issue for deep-lung penetration, it is likewise relevant in extrathoracic, particularly nasal deposition. Nasal deposition (as part of the extrathoracic deposition shown in Figure 1b) also exhibits a U-shape deposition pattern (ICRP, 1994, Hofman, 2011) and contributes to the observed U-shaped pattern for total deposition. While deposition fractions in the trachea-bronchial region form in the micron-size range is obviously related to the inertial properties of coarser aerosols, deposition in the nano-size range is less obvious. The latter is related to the turbulent flow regime in the nasal cavity and its associated high-filtering efficiency of small (and large) particles, which reduces inspiratory thoracic depositions of the ultrafine particle regime. Sedimentation dominates over impaction around the transition regime and is characterized by a "saddle-like" depression in total deposition curve (Moeller et al., 2010). The reduced deposition properties with very small particles (<1 nm, not shown in the Figure below), is related to the gas-like character of picometer-sized aerosols.

Owing to these general considerations, the motivation to come up with a novel class of atomizers for therapeutic use should be much clearer as it hugely extends the therapeutic applications and also the potentials to treat medical conditions that are difficult to come by with existing aerosolizers.

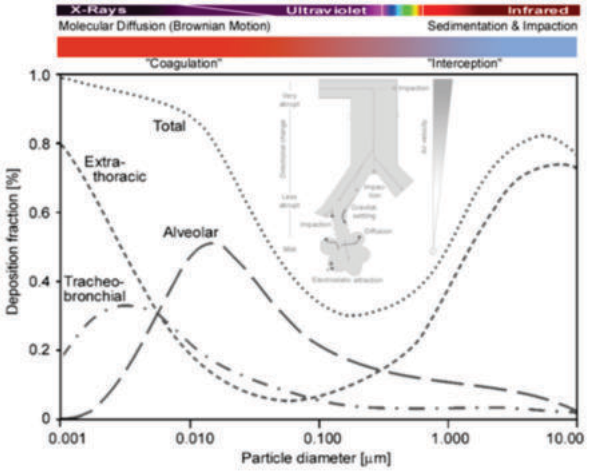

Fig. 1b: Normalized distribution of particle deposition for different regions of the respiratory tract system vs particle size. Subimposed the major deposition mechanisms for these regions. (modified after Madl, 2017).

A Compact, Small Size Aerosolizer

The current prototype -- already granted a valid patent status (Zarfl, 2019) – is based on the jet-venturi concept; however, with some significant differences, that regard the hydrodynamic properties in the aerosolization chamber. As can be seen in Figure 2, the nozzle is quite small, its overall dimensions measure just about 3 x 6 cm enabling about 6 mL of solution to be inserted into the nozzle. The nebulization is achieved via a pressurized hose inserted from the bottom of the nozzle, whereas the aqueous solution that needs to be aerosolized is inserted from the narrow side-port. The applied pressure induces vertical vortices within the septed chamber, which jerks out a tiny amount of the vortexed solution via the six apical orifices situated at the top. The body of the nozzle itself consists only of three sub-units: the upper and the lower casing into which the vortexing unit is slided into. Once these parts have undergone a routine sterilization procedure, the two outer subunits are inductively welded together, thereby forming a single body, whereas the proximal and side-inlets as well as the apical outlets are sealed with a peelable plastic-coated aluminum foil to assure sterility throughout the post-manufacturing handling procedure. As the nozzle was originally designed for in-situ placement into the nostrils of a horse (yet it was found that the nozzle is not just restricted to the field of veterinary medicine but more so for all medical applications including humans), general sterilization measures apply during laboratory and field preparation. Given these sterility aspects, the nozzle is ideal for a disposable, mono-usable device. For laboratory testing though, the authors refrained from theses sterilization measures in order to subject the atomizer for extensive performance tests, which are described in the methods section below. During these tests with various – both high and low viscosity – liquids, it became quickly clear that this device is suitable for both stationary as well as mobile applications, extending both the range of existing medical inhalators, especially hand-held aerosol puffers designed for potential drug administration via the lung rather than using the conventional oral, intra-venous, or sub-cutaneous pathways.

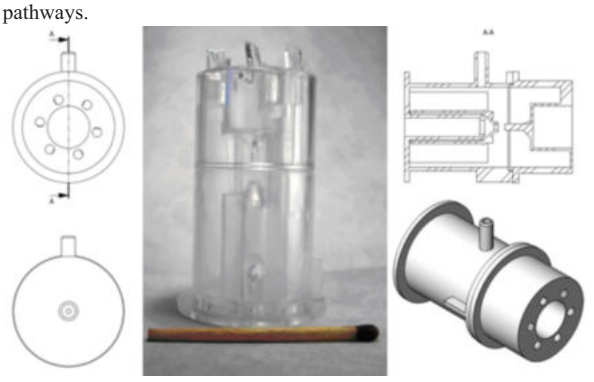

Fig. 2. CAD-drawings Of The Nozzle Along With A 3d-design And The Lasered 3d-printed Nozzle In Acrylic Glass. The Match Below Gives A Rough Idea About Its Overall Dimensions.

Methods

Sample preparation: Using a syringe, approximately 1.5 mL of a 0.2 % dexamethasone solution (Rapidexon, Richter Pharma, Wels) was injected via the side-port into the nozzle. In order to assure that proper vortices are formed within the nozzle, it is essential to gently swivel the nozzle assuring that it is not tilted and maintained in a vertical position.
Setup: Aerosolization efficiency was done using the setup as shown in Figure 2. Fitting the nozzle with a rubber interface O-ring it was possible to insert the nozzle (along with the pressurized hose) into the bottom opening of the premixing chamber. A portable compressor (model MP1 with a built-in HEPA-capsule, from MedicNano, not shown) provided the required nominal aerosolization pressure (2.5 bar) for as long as the system was programmed for, here 120 s (corresponds to half the measurement cycle of an SMPS run for the particle window between 5.5-350 nm). The compressor can be operated remotely in order to properly trigger the aerosolization event for the preset duration, which was set to comply with the SMPS sampling cycle (typically 4 mins)l i.e. it was found that atomization time exceeding 120 seconds lead to an overloading of both the premixer and the aerosol measurement chamber resulting in unfavorable effects leading to accelerated aerosol agglomeration, which in turn speeds up sedimentation rates and rapid decay of aerosol concentration within the measurement chamber.

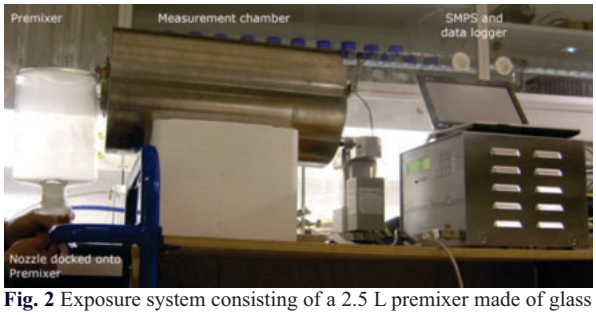

Fig. 2 Exposure system consisting of a 2.5 L premixer made of glass and a 22 L main steel chamber. The particle scanner is attached at the proximal end of the main measurement chamber.

The system itself is essentially a scaled-up version of a metered dose inhaler (Smith et al., 2005) with the only exception that instead of the liquified propellant a stand-alone pressure generator was used. This arrangement was chosen to allow the highly dynamic nebulized fraction (visible in the premixer) to stabilize and to gradually fill the measurement chamber where the Scanning Mobility Particle Sizer (SMPS+C) is attached to. The particle scanner consists of two units, a Dynamic Mobility Analyzer (DMA, model 5400) and a Condensation

Particle Counter (CPC, model 5500, both from Grimm Aerosol Technik). Data logging of the system is achieved via a LabView® software package (version 2.3) that enables direct visualization of the aerosol size distribution over 45 channels, covering a size range from 5.2 to 351.3 nm. Data logging extended well beyond the timer setting used during the nebulization procedure, and was done for up to 25 mins after the first injection into the chamber ceased. Doing so ensures that the post-injection aerosol dynamics within the chamber becomes evident. The scanned aerosol concentration (at "T+0", "T+4" and "T+8 min") and the corresponding size distributions reflect the aerosol inventory inside the measurement chamber, which includes all wall effects and other losses due to the chosen configuration of the setup.

Conversion from number particle to mass concentration:

Given the fact that the system depicts the numerical aerosol concentration (in cm^{-3}) it is essential to also perform a conversion into mass concentration [$\mu g/m^3$]. This can be done either via the LabView® software package or manually using the following relation (Hinds, 2005). In either case, the mathematically applied conversion has its pitfalls as it assumes that the particle consist of an idealized sphere (with a given aerodynamic diameter) – which, in the case of the aqueous aerosols employed in this study is nonetheless sufficiently accurate. The mathematical approach is summarized by the following equation,

$$m_P = \rho_P \frac{\pi}{6} d_P^3 m_P = n_P \frac{\rho_P \pi}{6} d_P^3 m_P = n_P \frac{\rho_P \pi}{6} d_P^3$$

$m_{\downarrow}p = ((_{\downarrow}p \ ^{*}(^{*})/6 \ [d] \ _{\downarrow}p^{\uparrow}3 \quad 1$

whereby the particle mass (m_p) is calculated using the density of the "liquid" (r_p) multiplied with the particle diameter (d_p) cubed. Given that the low concentration of the dexamethasone solution, the density of the liquid droplet can be matched with good accuracy to that of water. Gravimetric measurements revealed that the amount of solution introduced into the atomizer nozzle prior and after aerosolization about 1 g of solution has become airborne.

Modeling Lung Deposition

The "T+0", "T+4", "T+8" min averages of the acquired data obtained during the atomization of the dexamethasone solution were fed into the stochastic asymmetric lung deposition model developed by Koblinger and Hofmann (1990) and Hofmann and Koblinger (1990, 1992). The term "stochastic" refers to the Monte Carlo method in which inspired particles are transported through a stochastic asymmetric lung structure. Upon encountering a bifurcation, the selection of the airways in which a singly particle becomes transported deeper and deeper into the lung follows a randomly selected sequence. Furthermore, the term "asymmetric" refers to the Y-shaped bifurcation unit, whereby a larger tube branches into asymmetrically dividing progeny tubes. Thus the model was published by the above mentioned authors under the acronym IDEAL (Inhalation, Deposition and Exhalation of Aerosols in the Lung) and allows to model the deposition and clearance of inhaled particles not only for the entire lung but also for each lung lobe. The location of individual airways within the lung relative to the trachea is denoted by airway generation numbers, whereby the trachea is allocated as generation "0" while the following generations (following each bifurcations) is described by an ascending number in generation. A human lung typically has 25 to 27 bifurcations and with the highest generation number, the terminal bifurcation ends with the alveolar sacs. In addition, the bronchial branches in relation to the trachea, are divided in two classes. As superimposed in Figure 5a, generations 1-15 represent the bronchial lung region (gas conduction function), whereas the generations above that represent alveolar lung area (gas exchange zone) whereas the transition zone (where both conducting and gas exchange function van be found) is denoted as the acinar region (Yeh & Schum, 1980). For additional features of the IDEAL model, the authors refer to the in-depth description given by Hofmann (2011).

The IDEAL code used here is an upgraded version and operates with 60 size classes to easily accommodate the 45 size bins used by the SMPS. Deposition of an inhaled particle is calculated by considering the fate of an individual particle (Lagrangian approach), which is contrasted by those models that model deposition of entire particle populations (Eulerian approach). Therefore, it is necessary to run the model at least with 10^3 runs in order to obtain a reliable prediction of i) the amount of particles deposited and ii) where in the lung these have been deposited (Hussain et al, 2012).

As deposition strongly depends on morphology, age, sex and respiration rate, key parameters need to be plugged into the input matrix of the model. In this study case, we referred to a person at rest and as such used a tidal volume of 750 mL (based on 3.3L adult lung volume) with a respiration time of 4 seconds per breath (resting rhythm, corresponds to 15 puffs per minute).

Given that the used dexamethasone solution is quite low in concentration (0.2 %), the density value used in the IDEAL model was set to a standard aerosol density of $\rho = 1\ g/cm^3$, which makes it possible to determine also particle mass deposition calculations for each generation.

Taking into account the supersaturated conditions in the lungs (relative humidity of almost 100 %) implies that hygroscopic effects altered aerosol diameters for as long as the aerosols reside in the respiratory tract, resulting in incorrect particle sizing (Knoch & Finlay, 2002). The resulting increase in droplet size has been taken into account by running the model with different humidity growth factors (HGF), such as x1 (original particle diameter), x2 (double) and x5 (5-fold increase in diameter). Given that only a HGF of 5 is realistic, only the results using this growth dynamics have been further considered in this study.

RESULTS

The overall aerosolization efficiency over the 120 sec confirmed the high rate of atomization obtained using the 0.2 % dexamethasone solution. Practically, the solution introduced into the nozzle weighed 22.05 g prior to atomization, whereas after atomization the remaining weight of the solution still inside the nozzle amounted to 21.01 g, implying that most of the 950 mg dexamethasone solution was made airborne, with some losses attributed to wall-effects. Table 1 shows the conversion efficiency, when by assuming that the bulk of the mass difference was converted into the gaseous phase.

Table 1: Numeric Summary Of The Aerosol Inventory As Detected With The SMPS Within The Measurement Chamber

	Total	Mode	Median	Arith. Mean	Geom. Mean	Geom. St. Dev.
[min]		[nm]	[nm]	[nm]	[nm]	[nm]
dN	[ccm^{-3}]					
T+0	$5.416 \cdot 10^6$	68.50	88.20	102.10	86.00	1.91
T+4	$0.856 \cdot 10^6$	112.05	111.57	120.72	103.18	1.97
T+8	$0.297 \cdot 10^6$	124.19	123.72	132.13	118.77	1.68
dM	[$\mu g/m^3$]					
T+0	6654.58	214.63	195.81	205.45	188.50	1.54
T+4	1433.88	241.42	202.91	207.95	193.14	1.49
T+8	590.26	243.24	200.53	211.04	197.23	1.46

Each of the depicted trends in Figure 4a consists of 9 individual measurements out of which the last and the ninth are ignored by the labview®-based logging routine, leaving seven individual measurements which are then averaged to yield the scans visible in the graph. The time stamp "T+0" denotes the injection time ("0": injection within the first minute of sampling), with subsequent scans representing averages as measured after 4 mins and 8 mins respectively. Given that injection time was limited to 120 secs the injected aerosol puff is highly dynamic (particularly at "T+0" – visible via the error bars in figure 4a). The quasi poly-modal distribution stretching from approx. 50-130 nm underlines the instability of the sampled aerosol spectra and renders the sampling procedure with an SMPS a challenging task. The subsequent scans at "T+4 & T+8 mins" represents an "aging" aerosol, whereby the smaller particle fraction homogeneously agglomerate on the larger siblings, thereby rendering these spectral distributions far more stable. Nonetheless, all three scans reveal that the dominant particle fraction – even for the "aging" aerosols – are grouped in the nm-size range peaking at 5, 110 and 125 nm respectively. A stable equilibrium would be reached only once agglomeration has ceased and particle sedimentation becomes the dominating cleansing mechanism.

Using the input terms as obtained in figure 4a along with equation 1 it is possible to convert the numeric aerosol concentration into the corresponding mass equivalent. Doing so, it becomes obvious that the conversion from particle number to mass concentration highlights the cubic dependency, which translates into few larger particles dominating the size spectrum thereby obscuring the bulk of smaller-sized particles – as shown in Figure 4b. Since mass concentration does not correlate with the prevalence of respiratory diseases, while number concentration does (Hinds, 2005) – the same holds true for particle deposition of aerosolized therapeutics – makes clear why number

concentration should be prioritized over mass concentration.

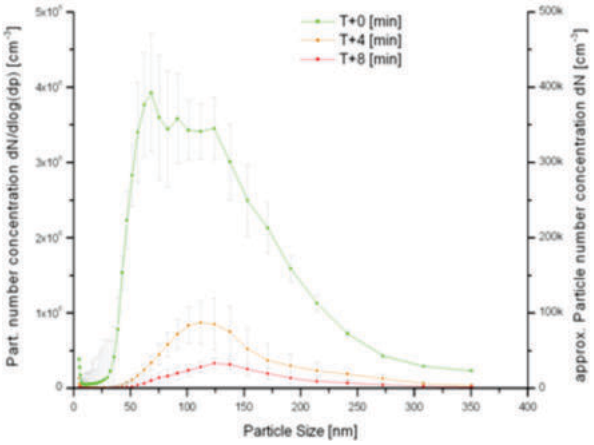

Fig.4a: Distribution Of Particle Number Concentrations And Its Evolution Over Time.

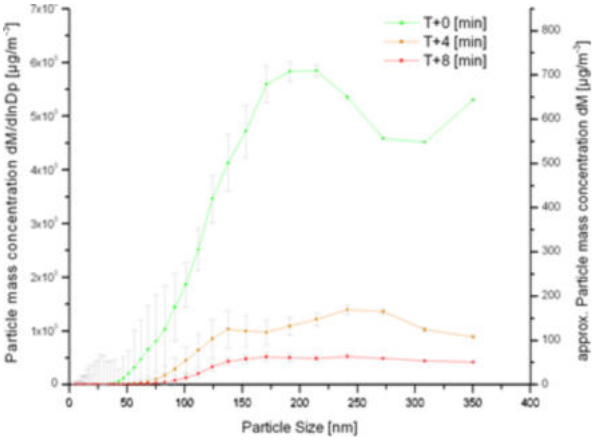

Fig.4b: Corresponding Distribution Of Particle Number Concentrations Converted Into Particle Mass Concentrations And Its Evolution Over Time.

However, not all of the inhaled particles will eventually deposit in the respiratory tract. Inhalability is therefore not identical to respirability. The inhalable fraction is defined as the original volume of air inhaled that enters the nose or mouth and is typically <1 (Hinds, 2005). Its determination can only be achieved empirically. Furthermore, in the very fine particle size classes diffusion properties dominate, which often translates into hardly any deposition. These particles are inhaled with the bolus of air but become expelled again as the bolus leaves the pulmonary region during exhalation (Hofmann, 2011). As both the inhalable fraction and the sub-nm-fraction are not relevant for deposition modelling, the IDEAL code only takes into account the respirable fraction in the size range >1 nm all the way to 350 nm (arbitrarily set upper limit as predetermined by the SMPS-output file – however, the code is capable of handling even 60 size bins with an arbitrarily set upper cut-off diameter at 60 µm).

Plugging the sampled aerosol datasets shown in figure 4a into the deposition model (IDEAL) yields the deposition fraction of such an inhaled aerosol. In the corresponding Figures 5a-d, the ordinate is the frequency of counting and as a dimensionless quantity (if multiplied with 100) denotes the deposition percentage; i.e. the maximum achievable deposition value cannot exceed "1" or 100 %. Given the high relative humidity within the pulmonary regime (i.e. 100 %), induces homogeneous particle agglomeration, thus resulting in net particle diameter growth. Accordingly, and in order to accommodate this particle growth induction, the simulation was set to a hygroscopic growth factor (HGF) of 5, as reproduced in Figure 5a and b. Therein, the diagram's abscissa represents the lung generation, with the trachea being assigned generation "0", the bronchial bifurcation tree constituting generation "1" to roughly "10" followed by the acinar region (mix of bronchial and alveolar structures) covering generations "11-16" and subsequently fading over to the alveolar regime as one steadily proceeds to higher generation numbers.

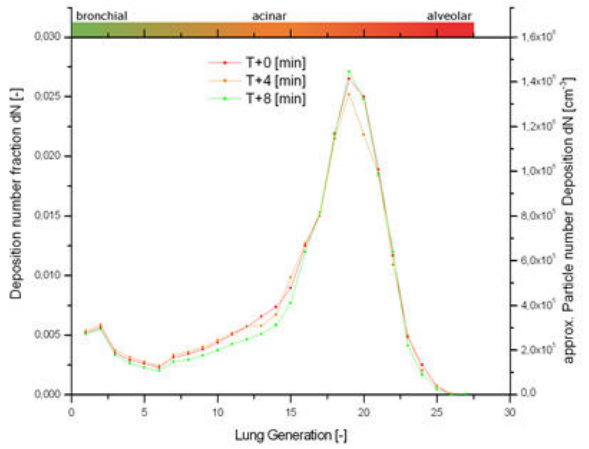

Fig.5a: Simulated lung particle deposition after T+0, 4, 8 mins after the aerosol injection into the system at an applied HGF of 5. The upper abscissa depicts the corresponding anatomical regime of the human pulmonary structure.

The deposition pattern shown in Figure 5a reflects the deposited fraction as derived from the input terms depicted in Figure 4a.

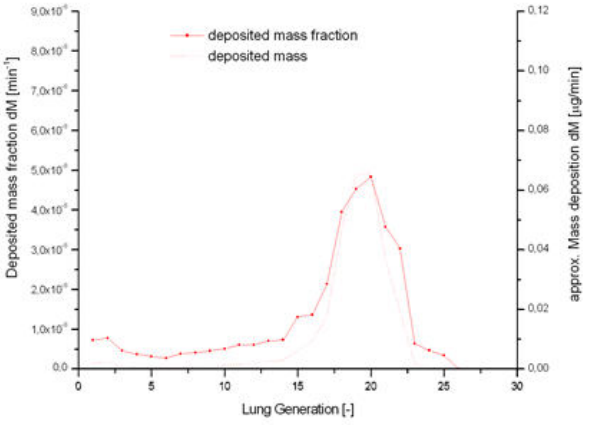

Fig.5b: Simulated Lung Mass Deposition After T+0 mins After The Aerosol Injection Into The System At An Applied HGF Of 5.

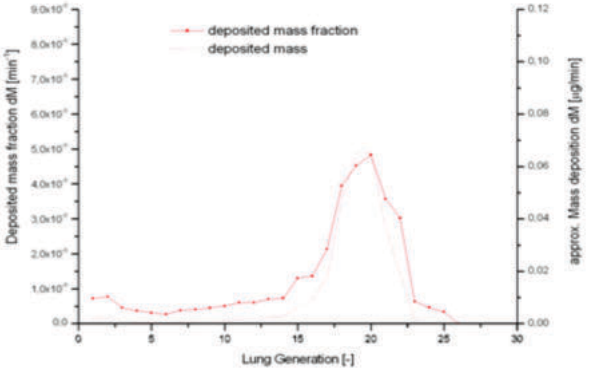

Fig.5c: Simulated lung mass deposition after T+4 mins after the aerosol injection into the system at an applied HGF of 5.

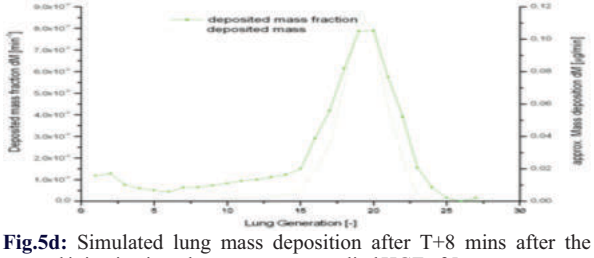

Fig.5d: Simulated lung mass deposition after T+8 mins after the aerosol injection into the system at an applied HGF of 5.

DISCUSSION

The distributions shown in Figure 4a (when plugged into the IDEAL code to simulate human particle lung deposition probabilities) clearly shows that the majority of the atomized fluid would penetrate deep into the lung. Based on the simulation, the extra-thoracic deposition in the nasopharynx covers a range from 4.76 to 5.97 % depending whether one refers to the first, second or third simulated puff. Given the lung-inherent relative humidity of 100 % and the associated homogenous particle growth leading to heavier droplets, which contributes to an increased deposition factor in the lungs compared to a hydrophobic aerosol of the same density and size distribution (data not shown). Based on the simulation model, a significantly high proportion of the generated aerosol (peaking around 100 nm) easily penetrates the alveolar regime, with deposition peak values around the 19th lung generation. The overall deposition maximum within the lungs that can be achieved using the IDEAL code amounts to 25.6 to 26.5 % for the three simulated aerosol puffs.

Unlike other aerosolizers the range of measured particle diameter fits rather good in the range of the generic diagram shown in Figure 1b, in which extra-thoracic, tracheobronchial, and pulmonary (alveolar) deposition are depicted separately over the plotted particle diameter range stretching from 1 nm to 10 µm, making this nozzle a highly efficient low-dose inhalation device. Such a feature opens new perspectives for multiple medical indications of bronchial and lung treatment in humans (with a particular focus on COPD) as well as in animals. The collected data yield deposition characteristic and deposition rate (approx. 26 % in the measured device compared to most devices falling short to reach even 5 %).

Further benefits of the used aerosolizer concern aspects like i) no extra breathing technique on behalf of the proband required to increase penetration depth to reach deeper areas of the lung; ii) both nose and mouth breathing can be employed and iii) prototypes implementing this nozzle into a portable battery-powered unit showed that It can be converted into a palm-size device without significant losses in aerosolization efficiency. Moreover, currently used aerosolizers have a focus on the mass term rather than on the numeric quantity, thus exposure to therapeutic agents is usually quantified in the overall deposited mass, neglecting the benefits of high particle numbers and their small sizes (directly correlated to lung penetration efficiency) in order to obtain the same mass deposition equivalent as in conventional approaches. An essential drawback in deposition methods focusing on mass is depicted in Figure 1b whereby interception of heavy particles (due to the cubic relationship as shown in Eq. 1) results in a huge fraction of the therapeutic substance lost as a result of impaction even before reaching the intended target region of the lung; i.e. being deposited in the oro-/naso-pharyngal and trachea-bronchial region. It has been estimated that only 10 % of the dose that is initially placed in the conventional nebulizer will be effectively deposited in the region of interest (O'Callaghan & Barry, 1997). In consensus, the particle size of most aerosolizers intended for inhalation is set to the µm-scale, resulting in rather low lung deposition rates. With regards to the obtained data with dexamethasone, it is now possible to state that the novel design of the nozzle as shown in Figure 2 (which is the result of numerous design modifications) finally yields very satisfying aerosolization results that are reflected in optimized deposition characteristics. This holds valid for any drug with analogous concentrations as it would reveal similar deposition properties. In extreme cases – as observed with highly viscous liquids such as olive oil (results merit a separate publication, thus not shown) along with tits hydrophobic properties (HGFx1) – reveal altered deposition properties in that deposition probability is slightly shifted to lower lung generation numbers.

Given these features, we are confident that this aerosolizer represent a new stepstone to increase aerosolization efficiency and at the same time lower the amount of therapeutic agents used to minimize adverse side-effects from overdosing often encountered in conventional devices.

REFERENCES

1. Adjei AL (2002) The Pressurized Metered-Dose Inhaler. In: Rathbone MJ, Hadgraft J, Roberts MS (eds). Modified-release drug delivery technology. Dekker, New York (USA). ISBN: 0-8247-0869-5
2. Berlinski A, Willis JR (2013) Albuterol delivery by 4 different nebulizers placed in 4 different positions in a pediatric ventilator in vitro model. Respir Care. 58(7): 1124-33. doi: 10.4187/respcare.02074
3. Christensen HM, Driver OGA (2021) The fractal nature of clouds in global storm-resolving models. Geophysical Research Letters, 48, e2021GL095746. doi: 10.1029/2021GL095746
4. Hickey AJ, Swift D (2001) Measurement of Pharmaceutical and Diagnostic Aerosols. In: Baron PA, Willeke K (eds) Aerosol Measurement, 2nd ed. Wiley Interscience, Toronto (CDN). ISBN: 0-471-35636-0
5. Hickey AJ (2002) Molecular-Weight Molecules as Aerosols. In: Rathbone MJ, Hadgraft J, Roberts MS (eds). Modified-release drug delivery technology. Dekker, New York (USA). ISBN: 0-8247-0869-5
6. Hinds CW (2005) Aerosol Properties. In: Ruzer LS, Harley NH (eds) Aerosols handbook: measurement, dosimetry, and health effects. CRC Press, Boca Raton (USA). ISBN: 1-56670-611-4
7. Hofmann W, Koblinger L (1990). Monte Carlo Modeling of Aerosol Deposition in Human Lungs. Part II: Deposition Fractions and Their Sensitivity to Parameter Variations. J. Aerosol Sci. 21: 675–688. doi: 10.1016/0021-8502(90)90122-E
8. Hofmann W, Koblinger L (1992) Monte Carlo modeling of aerosol deposition in human lungs. Part III: Comparison with experimental data. J Aerosol Science, 23(1): 51-63. doi: 10.1016/0021-8502(92)90317-O
9. Hofmann W (2011). Modelling inhaled particle deposition in the human lung – A review. Journal of Aerosol Science, 42(10): 693-724. doi: 10.1016/j.jaerosci.2011.05.007
10. Hussain M, Madl P, Hofmann W, Khan A (2012). Implementation of charged particles deposition in a stochastic lung model and calculation of enhanced deposition, Aerosol Science and Technology, 46(5): 547-554. doi: 10.1080/02786826.2011.645957
11. ICRP (1994) Human Respiratory Tract Model for Radiological Protection. International Commission on Radiological Protection Publication 66, Annals of ICRP 24, Nos. 1–3. Pergamon Press, Oxford (UK). ISBN 0-08-041154-1
12. Knoch M, Finlay W (2002) Nebulizer Technologies. In: Rathbone MJ, Hadgraft J, Roberts MS (eds). Modified-release drug delivery technology. Dekker, New York (USA). ISBN: 0-8247-0869-5
13. Koblinger L, Hofmann W (1990). Monte Carlo Modeling of Aerosol Deposition in Human Lungs. Part I: Simulation of Particle Transport in a Stochastic Lungs Structure. J. Aerosol Sci. 21: 661–674. doi: 10.1016/0021-8502(90)90121-D
14. Lutgens KF, Tarbuck EJ (2010) The Atmosphere: an Introduction to Meteorology, 11th ed. Prentice Hall, New Jersey (USA), ISBN: 0-3215-8733-2
15. Madl P, Del Giudice E, Voeikov VL, Tedeschi A, Kolarž P, Gaisberger M, Hartl A (2013) Evidence of Coherent Dynamics in Water Droplets of Waterfalls. WATER 5: 57-68. doi: 10.14294/WATER.2013.7
16. Madl P (2017) Aerosols – Tiny but Powerful. Lecturing script, Paris Lodron University of Salzburg, available online (accessed: May, 2022): https://biophysics.sbg.ac.at/talk/trott-2012.pdf
17. Madl P (2012) Exposure to Nano-Sized Particles and the Emergence of Contemporary Diseases with a Focus on Epigenetics, Ch.14. In: Khare M (ed) Air Pollution - Monitoring, Modelling and Health. InTech Publ. (HR). doi: 10.5772/1801
18. Moeller W, Kreyling WG, Schmid O, Semmler-Behnke, Schulz H (2010) Deposition, Retention and Clearance, and Translocation of Inhaled Fine and Nano-Sized Particles in the Respiratory Tract. In: Gehr O, Muehlfeld C, Rothen-Rutishauser B, Blank F (eds). Particle-Lung Interactions, 2nd ed. ISBN: 1-4200-7256-0
19. O'Callaghan C, Barry PW (1997) The science of nebulized drug delivery. Thorax, 52 (Suppl 2): S31-S44. doi: 10.1136/thx.52.2008.s31
20. Rosell-Llompart J, Grifoll J, Loscertales IG (2018). Electrosprays in the cone-jet mode: From Taylor cone formation to spray development. Journal of Aerosol Science, 125: 2-31. doi: 10.1016/j.jaerosci.2018.04
21. Smith HDC, Garcia-Conteras L, Cooney DJ, Garmise RJ, Jones LD, Hickey AJ (2005) Medical and pharmaceutical aerosols. In: Ruzer LS, Harley NH (eds) Aerosols handbook: measurement, dosimetry, and health effects. CRC Press, Boca Raton (USA). ISBN: 1-56670-611-4
22. Sorino C, Negri S, Spanevello A, Visca D, Scichilone N (2020). Inhalation therapy devices for the treatment of obstructive lung diseases: the history of inhalers towards the ideal inhaler. European Journal of Internal Medicine. doi: 10.1016/j.ejim.2020.02.023
23. Telko MJ (2009) Investigation of Electrostatic Charging Phenomena in Dry Powder Inhalers and the Effect on Deposition. PhD-Thesis, University of North Carolina at Chapel Hill, NC, USA
24. Yan Y (2001) Some Applications of Biophoton Measurements. 10th Summerschool at the International Institute of Biophysics, Neuss, FRG
25. Yeh HC, Schum GM (1980) Models of human lung airways and their application to inhaled particle deposition. Bull Math Biol. 42(3): 461-80. doi: 10.1007/BF02460796.
26. Young FR (1999) Cavitation. Imperial College Press, London (UK). ISBN: 1-8609-4198-2
27. Zarfl HP (2019), Aerosol Dispenser. US Patent D856140. Available online (accessed May, 2022): https://patft.uspto.gov/netahtml/PTO/srchnum.htm